A mathematical model of cartilage regeneration after cell therapy

Michael Lutianov, Shailesh Naire, Sally Roberts, Jan-Herman Kuiper

A mathematical model of cartilage regeneration after cell therapy

Michael Lutianov, Shailesh Naire, Sally Roberts, Jan-Herman Kuiper

PII: S0022-5193(11)00402-4
DOI: doi:10.1016/j.jtbi.2011.08.007
Reference: YJTBI 6579

To appear in: *Journal of Theoretical Biology*

Received date: 9 February 2011
Revised date: 23 June 2011
Accepted date: 6 August 2011

Cite this article as: Michael Lutianov, Shailesh Naire, Sally Roberts and Jan-Herman Kuiper, A mathematical model of cartilage regeneration after cell therapy, *Journal of Theoretical Biology*, doi:10.1016/j.jtbi.2011.08.007

A Mathematical Model of Cartilage Regeneration after Cell Therapy

Michael Lutianov*[,a], Shailesh Naire[b], Sally Roberts[c], Jan-Herman Kuiper[a,c]

[a] *Institute of Science and Technology in Medicine, Keele University, Keele, ST5 5BG, U.K.*

[b] *School of Computing and Mathematics, Keele University, Keele, ST5 5BG, U.K.*

[c] *Robert Jones and Agnes Hunt Orthopaedic & District Hospital NHS Trust, Oswestry, SY10 7AG, U.K.*

Abstract

Autologous Chondrocyte Implantation (ACI) is a cell-based therapy used mainly for the treatment of chondral defects in the knee. It involves surgically inserting isolated chondrocytes or mesenchymal stem cells (MSCs), previously expanded in culture, into the defect region. These chondrocytes then proliferate and migrate, in the process forming extracellular matrix (ECM) and new cartilage. In the case of MSCs, the process of forming new cartilage is initiated only after differentiation of the stem cells into chondrocytes. Many details of the repair process following insertion in humans are unknown. To enable better understanding of the repair process, we present a mathematical model of cartilage regeneration after cell therapy. The key mechanisms involved in the regeneration process are simulated by modelling cell migration, proliferation and differentiation, nutrient diffusion and depletion, and ECM synthesis and degradation at the defect site, both spatially and temporally. The model successfully simulates the progression of cartilage regeneration. The model predicts a time frame of about 18 months for the defect to reach full maturation which corresponds with results from clinical studies and demonstrates that cartilage regeneration is a slow process. Moreover, the model also suggests that regeneration using stem cells alone is no better than that using chondrocytes. The stem cells need to first differentiate into chondrocytes before forming ECM and new cartilage, a process that is initiated only after the stem cell density exceeds a threshold value. Furthermore, with chondrocytes alone, the matrix seems to develop from the subchondral bone interface as compared to the normal cartilage interface, in the case of stem cells alone. The influence of initial conditions and parameters, such as the initial cell seeding densities and cell proliferation rates, are shown to not significantly influence the general evolution characteristics other than accelerating the initial growth process. The model presented here is a first approach towards better understanding of cartilage regeneration after cell therapy techniques.

Key words: stem cells, chondrocytes, defect, cartilage.

1. Introduction

Articular cartilage is avascular, aneural and sparsely populated by cells. This limits its capacity for self-repair in cases of carilage damage due to, for example, arthritis or trauma. Surgical treatment is often necessary to encourage repair and avoid any long-term problems. One such treatment and the focus of this study is Autologous Chondrocyte Implantation (ACI). ACI is a cell-based therapy used mainly for the treatment of chondral defects in the knee. ACI has been in clinical use since 1987 and has been performed on over 12000 patients worldwide (Marlovits et al. (2006)). The ACI therapy involves, first, isolating chondrocytes from an arthoscopic harvest of a biopsy of healthy cartilage, culturing them over a period of weeks and then surgically inserting them into the damaged (or defect) region (Brittberg (2008)). Bone marrow-derived

*Author to whom correspondence should be addressed. email: m.lutiyanov@istm.keele.ac.uk

mesenchymal stem cells (BMSCs) have also been used in this therapy, instead of chondrocytes, due to their capacity to differentiate into different cell types (Nejadnik et al. (2010)). In this paper, we refer to this therapy Articular Stem cell Implantation (ASI).

Figures 1(a),(b) show a cartilage defect in the knee and a schematic of the defect cross-section, respectively. The length of the defect is about 10-20mm and its thickness is about 2-3mm. After debridement of the defect, chondrocytes or MSCs are seeded along the defect walls. The initial number of cells seeded are in excess of a million. The chondrocytes proliferate (by taking-up nutrients) and migrate, in the process forming

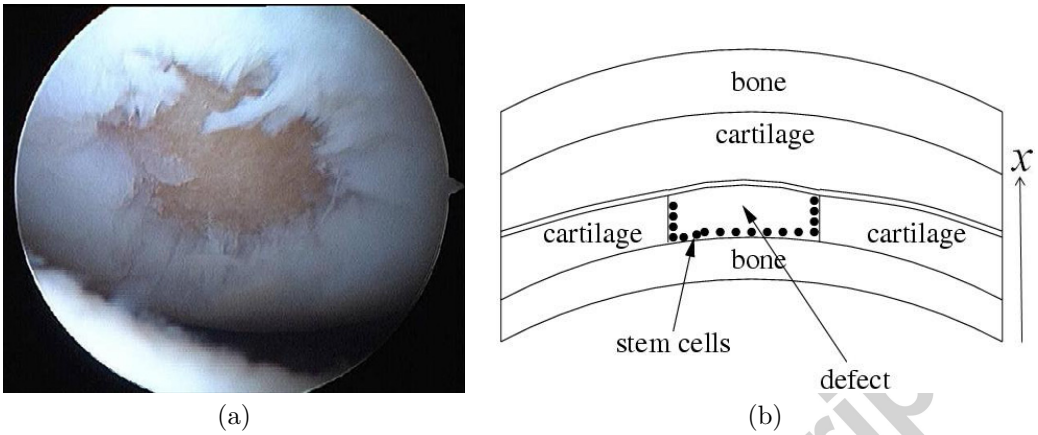

Figure 1: (a) Cartilage defect in the knee; (b) schematic of a cross-section of the defect shown in (a). The axis denoted by x in (b) is along the thickness of the defect. After debridement of the defect, either chondrocytes or mesenchymal stem cells are seeded along the defect walls.

ECM and new cartilage. In the case of MSCs, the process of forming new cartilage is initiated only after the stem cells first differentiate into chondrocytes. The mechanical loading environment is also essential since it can modulate the cell proliferation, differentiation and migration rates thereby influencing the production of ECM and hence the tissue's overall structure (Darling et al. (2000)). Similarly, growth factors, such as those from the transforming growth factor-beta (TGF-β) superfamily, e.g. TGF-β1, and basic fibroblast growth factor, FGF-1 and FGF-2, are known to enhance chondrogenesis and cartilaginous tissue formation *in vitro* (Jakob et al. (2001)). They modulate the secretion of certain molecules from different cells and regulate a wide range of cell activities including migration, proliferation and differentiation.

Many details of the repair process following cell insertion in humans are unknown and the only detailed data currently available is the condition of the cartilage studied on small biopsies obtained approximately a year after cell implantation (Roberts et al. (2003)). Animal models do however provide some insight in the repair process (Ahern et al. (2009)). The structural composition of the resulting reparative tissue plays an important role in characterising the success of the repair (Vavken et al. (2010)). However, much remains unknown about the influence of various cell-related aspects on the development of tissue. Theoretical biology can significantly contribute in further unraveling the interactions between the different influencing factors.

Considerable research effort has been devoted in the development of theoretical models for tissue growth and repair. Although the vast literature on tissue growth and repair has mainly dealt with experimental analysis, there are numerous mathematical models that have been developed to model the various biological processes involved. These range from discrete models (where a few thousand cells are involved) to continuum models (in excess of a few million cells involved). For the problem in consideration here, the initial seeding of cells in the defect is quite large. A continuum approach is therefore appropriate to model their growth. The continuum models generally take the form of a system of reaction-diffusion-type equations, where cell migration is modeled as a diffusive process, and cell proliferation, differentiation and death are represented by reaction terms. Tissue-related continuum models that are closely related to the problem described here are in wound healing (Sherratt et al. (1990)), and angiogenesis in both tumor growth (Levine et al. (2001);

McDougall et al. (2002)) and wound healing (Pettet et al. (1996); Olsen et al. (1997)). Also, closely related to cartilage repair are theoretical models of fracture healing. The role of growth factors in fracture healing was modeled by Bailón-Plaza and Van Der Meulen (Bailón-Plaza et al. (2001)). Mathematical models investigating the role of the mechanical loading environment in regulating cartilage repair was done by Prendergast and co-workers (Kelly et al. (2005)). Mathematical models simulating the *in vitro* growth of engineered cartilage have also been investigated (Galban et al. (1997); Galban et al. (1999); Obradovic et al. (2000)). These models, along with cell growth, also account for the consumption of nutrients (mainly oxygen) essential for the cells to grow and proliferate. Factors influencing the oxygen concentration gradient in articular cartilage (from cartilage to bone interface) have been determined experimentally and modelled mathematically by Urban and co-workers (Zhou et al. (2004); Zhou et al. (2007)). Since articular cartilage is avascular, both nutrient supply and waste removal rely on diffusion. One-dimensional reaction-diffusion models of nutrient transport were developed to predict the oxygen tension profile across articular cartilage as a function of cartilage thickness and cell density.

To the best of our knowledge, we are not aware of any previous theoretical models related to ACI therapy. Nevertheless, the above continuum modelling approach can be adapted to model this situation. Here we use a similar approach as in Olsen *et al.* (Olsen et al. (1997)) for wound healing and Bailón-Plaza and Van Der Meulen (Bailón-Plaza et al. (2001)) for fracture healing. Our modelling framework focusses on ECM production due to chondrocyte/stem cell migration and proliferation, and stem cell differentiation into chondrocytes. Cell proliferation and differentiation is modulated by the amount of nutrients available. Cell migration, proliferation and differentiation, nutrient diffusion and depletion, and ECM synthesis and degradation are modeled and simulated at the defect site, both spatially and temporally. The model is then used to investigate the effects on cartilage regeneration (using ECM production levels as a marker) of the initial seeding densities and parameters, such as cell proliferation/differentiation rates. The model presented here is a first approach towards understanding cartilage regeneration after cell therapy.

The plan of the paper is as follows. §2 describes the basic model and the assumptions made, the boundary and initial conditions used, estimates of the parameter values and the scalings used to non-dimensionalize the equations. §3 shows the results of simulations for two initial seeding protocols; one in which only chondrocytes are seeded (relevant to ACI therapy) into the defect and the other in which only stem cells are seeded (relevant to ASI therapy). Results showing sensitivity to certain parameters are also shown here. Finally, §4 discusses the implications of the model results on ACI therapy and future work.

2. Mathematical model

2.1. Model formulation

A typical cartilage defect has small aspect ratio, i.e., its length and width are much larger than its thickness depth, see Figure 1. This enables us to simplify to a one-dimensional problem where we model cell growth along the defect thickness only. The variables in our model are: the stem cell number density, C_S, the chondrocyte number density, C_C, the nutrient concentration, n, and the matrix density, m. Cell density is measured in number of cells per unit volume, matrix density is measured as mass per unit volume and nutrient concentration is measured in number of moles per unit volume.

We now develop a mathematical model for the evolution of each species in time, t, and space, x, where x is measured along the thickness of the defect (see Figure 1). We use simple proportionality relationships to model the rate of change of each species. The stem cell density is considered first and is described in detail. The evolution of the other species follow using similar arguments.

Stem cells can proliferate by uptake of nutrients, they can migrate (or diffuse) and can differentiate into

chondrocytes. Based on these processes, the rate of change of stem cell density is modelled as

$$\frac{\partial C_S}{\partial t} = \frac{\partial}{\partial x}\left(D_S(m)\frac{\partial C_S}{\partial x}\right) + p_1\left(m, \frac{C_S}{C_{S,max}(m)}\right) C_S \frac{n}{n+n_0} H\left(n-n_1\right) - p_2 C_S H\left(C_S - C_{S_0}\right) - p_3 C_S H\left(n_1 - n\right). \tag{1}$$

The first term on the right of Eq. (1) represents random stem cell migration, modelled as a diffusion process, with stem cell diffusion coefficient, D_S. This coefficient is assumed to depend on the matrix density, m. This is based on the argument that cells can only migrate by attaching to a substrate (in this case, matrix). We follow Olsen et al. (1997) and Bailón-Plaza et al. (2001) and choose

$$D_S(m) = D_{S_0}\frac{m}{m^2 + m_1^2}, \tag{2}$$

so that $D_S = 0$ when $m = 0$, $D_S \to 0$ for large m and D_s attains a maximum at some intermediate matrix density, $m = m_1$. The coefficient, D_{S_0}, is chosen such that, $D_{S_0} = 2m_1 D_S$, where D_S is the maximum stem cell migration (or diffusion) rate (Bailón-Plaza et al. (2001)). We choose m_1 such that, $0 < m_1 \ll m_{max}$, where m_{max} is a maximum matrix density.

The second term on the right of Eq. (1) represents stem cell proliferation (cells are being formed, hence the positive sign in front of this term). Cell proliferation is assumed to be proportional to the stem cell density and the nutrient concentration. This process is assumed to start only when the nutrient concentration exceeds a critical value, n_1 (or, alternatively, cell proliferation is switched-off when the nutrient concentration falls below this critical value). This is modelled by the Heaviside function, $H(n-n_1)$, which takes the unit value when $n > n_1$ and zero otherwise. The nutrient concentration, n_0, is a threshold concentration above which the rate of change of stem cell density due to proliferation saturates to a constant value. The stem cell proliferation rate is given by p_1. The proliferation rate is assumed to depend on both the stem cell and matrix densities. We choose

$$p_1\left(m, \frac{C_S}{C_{S,max}(m)}\right) = A(m)\left(1 - \frac{C_S}{C_{S,max}(m)}\right), \quad A(m) = p_{1_0}\frac{m}{m^2 + m_2^2},$$
$$C_{S,max}(m) = C_{S,max_0}\left(1 - \frac{m}{m_{max}}\right). \tag{3}$$

The dependence of p_1 on the matrix density (represented by $A(m)$) is chosen so that $p_1 = 0$ when $m = 0$, $p_1 \to 0$ for large m and p_1 attains a maximum at some intermediate matrix density, $m = m_2$. The coefficient, p_{1_0}, is chosen such that, $p_{1_0} = 2m_2 p_1$, where p_1 is a maximum stem cell proliferation rate. We choose m_2 such that, $0 < m_2 \ll m_{max}$. The dependence of p_1 on the stem cell density is assumed to follow a logistic growth model with the proliferation rate decreasing as the stem cell density approaches its maximum value, $C_{S,max}$. This maximum stem cell density is assumed to depend on the matrix density as shown above. This is interpreted as follows. The maximum space available for the stem cells to proliferate at any location is modulated by the matrix density there ($C_{S,max}$ is assumed to decrease linearly with increasing m). Here, C_{S,max_0} is a reference maximum stem cell density.

The third term on the right of Eq. (1) models stem cell differentiation (cells are being depleted, hence the negative sign in front of this term) into chondrocytes and is assumed to be proportional to the stem cell density. It is assumed that the differentiation process begins once the stem cell density, at any location, exceeds a threshold density, C_{S_0} (see, for example, DeLise et al. (2000), Mankani et al. (2007)). This is modelled using the Heaviside function, $H(C_S - C_{S_0})$, which takes the unit value when $C_S > C_{S_0}$ and zero otherwise. This is a crude way of modelling the onset of stem cell differentiation. The stem cell differentiation rate (or chondrocyte formation rate from stem cell differentiation) is given by p_2, and is assumed constant.

The last term in Eq. (1) represents cell death due to lack of sufficient nutrients. This process starts when the nutrient concentration falls below the critical value, n_1, and is modelled using the Heaviside function,

$H(n_1 - n)$, which takes the unit value when $n < n_1$ and zero otherwise. The cell death rate is p_3, and is assumed constant.

Similar to the above, the rate of change of chondrocyte density is written as

$$\frac{\partial C_C}{\partial t} = \frac{\partial}{\partial x}\left(D_C(m)\frac{\partial C_C}{\partial x}\right) + p_4\left(m, \frac{C_C}{C_{C,max}(m)}\right) C_C \frac{n}{n+n_0} H\left(n - n_1\right) + p_2 C_s H\left(C_S - C_{S_0}\right) - p_5 C_c H\left(n_1 - n\right), \tag{4}$$

where D_C is the chondrocyte migration (diffusion) coefficient, p_4 is the chondrocyte proliferation rate and p_5 is the chondrocyte death rate. We use similar expressions as in Eqs. (2,3) for

$$\begin{aligned} &D_C(m) = D_{C_0}\frac{m}{m^2 + m_1^2}, \;\; p_4\left(m, \frac{C_C}{C_{C,max}(m)}\right) = B(m)\left(1 - \frac{C_C}{C_{C,max}(m)}\right), \\ &B(m) = p_{4_0}\frac{m}{m^2 + m_2^2}, \;\; C_{C,max}(m) = C_{C,max0}\left(1 - \frac{m}{m_{max}}\right). \end{aligned} \tag{5}$$

where D_{C_0} is chosen such that, $D_{C_0} = 2m_1 D_C$, D_C is the maximum chondrocyte migration (diffusion) rate and p_{4_0} is chosen such that, $p_{4_0} = 2m_2 p_4$, where p_4 is a maximum chondrocyte proliferation rate. The maximum chondrocyte density, $C_{C,max}$, is assumed to decrease linearly with matrix density, m. C_{C,max_0} is a reference maximum chondrocyte density. We choose the reference maximum stem cell and chondrocyte densities, C_{S,max_0}, C_{C,max_0}, respectively, such that $C_{S,max_0} + C_{C,max_0} = C_{total,max_0}$, where C_{total,max_0} is a reference maximum total cell density. Hence, using the expressions for $C_{S,max}$ and $C_{C,max}$ in Eqs. (3,5) gives, $(C_{S,max} + C_{C,max})(m) = C_{total,max_0}(1 - m/m_{max})$.

The rate of change of nutrient concentration is modelled as

$$\frac{\partial n}{\partial t} = D_n\frac{\partial^2 n}{\partial x^2} - \frac{n}{n+n_0}\left(p_6 C_S + p_7 C_C\right), \tag{6}$$

where D_n is the nutrient diffusion coefficient (assumed constant), p_6 and p_7 represent the nutrient uptake rate by stem cells and chondrocytes, respectively (assumed constant). The rate of change of matrix density is

$$\frac{\partial m}{\partial t} = D_m\frac{\partial^2 m}{\partial x^2} + p_8(m)\frac{n}{n+n_0}C_C, \tag{7}$$

where D_m is the matrix diffusion coefficient (assumed constant) and p_8 is the matrix synthesis rate. We choose

$$p_8(m) = p_{8_0} - p_{8_1} m, \tag{8}$$

where p_{8_0} is a matrix production rate and p_{8_1} is its degradation rate. This assumes that the matrix synthesis rate decreases linearly with increasing matrix density (Olsen et al. (1997), Bailón-Plaza et al. (2001)).

2.2. Boundary conditions

We need to specify two boundary conditions for each species. These are specified at either end of the defect domain. We choose $x = 0$ at the bottom (subchondral bone interface) and $x = d$ (normal cartilage interface) at its upper end. The boundary conditions at $x = 0$ are:

$$-D_S(m)\frac{\partial C_s}{\partial x} = f(t), \;\; -D_C(m)\frac{\partial C_c}{\partial x} = 0, \;\; -D_n\frac{\partial n}{\partial x} = 0, \;\; -D_m\frac{\partial m}{\partial x} = 0. \tag{9}$$

The first boundary condition represents a prescribed flux of stem cells, $f(t)$ (number of cells/mm^2/hr), diffusing into the defect from the subchondral bone. This implies that the subchondral bone has been perforated and the stem cells can migrate into the defect. We choose $f(t)$ such that, with time, the source

of stem cells diminishes implying regeneration of the subchondral bone. The remaining three boundary conditions represent no flux of chondrocytes, nutrients and matrix, respectively, from the underlying bone.

At $x = d$, we impose:

$$-D_S(m)\frac{\partial C_s}{\partial x} = 0, \;\; -D_C(m)\frac{\partial C_c}{\partial x} = 0, \;\; n = N_0, \;\; -D_m\frac{\partial m}{\partial x} = 0. \tag{10}$$

The first, second and fourth boundary conditions represent no flux of stem cells, chondrocytes and matrix, respectively, from the normal cartilage interface. We assume that a reservoir of nutrients with concentration, N_0, is always available at this end.

2.3. Initial conditions

We need to prescribe profiles for each species at time $t = 0$. We are mainly interested in two scenarios:

(a) The first scenario is related to Articular Stem cell Implantation (ASI). The initial conditions mimic the situation of an initial seeding of stem cells in the defect filled with nutrients with no chondrocytes and a small amount of matrix present. The initial conditions chosen for this case are:

$$C_s = C_S^{(0)}h(x), \;\; C_c = 0, \;\; n = N_0, \;\; m = m_3. \tag{11}$$

Here, $C_S^{(0)}$ and $h(x)$ are an initial stem cell density and profile, respectively, m_3 is some initial matrix density (assumed to be uniformly distributed in the defect). The initial nutrient concentration is uniform with value N_0.

(b) The second scenario is related to Articular Chondrocyte Implantation (ACI). Initially, chondrocytes are seeded into a nutrient-filled defect with no stem cells and a small amount of matrix present. The initial conditions chosen for this case are:

$$C_s = 0, \;\; C_c = C_C^{(0)}h(x), \;\; n = N_0, \;\; m = m_3. \tag{12}$$

Here, $C_C^{(0)}$ and $h(x)$ are an initial chondrocyte density and profile, respectively.

2.4. Non-dimensionalization

There are several parameters appearing in the model. Their estimated values and the references from which they are obtained are provided in Table 1.

It is instructive to non-dimensionalize (make dimensionless) the above equations, boundary and initial conditions. One can then compare (or measure) the variables against their corresponding characteristic quantities. We introduce the following dimensionless variables based on characteristic quantities for each variable:

$$\bar{x} = x/d, \; \bar{t} = t(p_{8_0}C_{total,max_0}/m_{max}), \; (\bar{C}_S, \bar{C}_C) = (C_S, C_C)/C_{total,max_0}, \; \bar{m} = m/m_{max}, \; \bar{n} = n/N_0, \tag{13}$$

where the overbars represent dimensionless quantities. The characteristic quantities used to measure the spatial variable, x, cell densities, matrix density and nutrient concentration are the defect thickness, d, the reference maximum total cell density, $C_{total,max0}$, the maximum matrix density, m_{max}, and the initial nutrient concentration, N_0, respectively. We choose to measure time, t, based on the matrix production time scale, $m_{max}/(p_{8_0}C_{total,max_0})$. Using the parameter values in Table 1, we estimate this time scale to be approximately 11 days. Henceforth, a unit of time corresponds to approximately 11 days.

dimensional parameters	estimated value
defect thickness, d	2-3 mm
maximum stem cell migration (or diffusion) coefficient, D_S	$3.6 \times (10^{-4}$ - $10^{-3})$ mm^2/hr (Obradovic et al. (2000))
maximum chondrocyte migration (or diffusion), coefficient, D_C	3.6×10^{-4} mm^2/hr (Obradovic et al. (2000))
stem cell migration (or diffusion), coefficient, $D_{S_0} = 2m_1 D_S$	$7.2 \times (10^{-9}$-$10^{-8})$ (mm^2/hr) (g/mm^3) (assuming $m_1 = 10^{-5}$ g/mm^3)
chondrocyte migration (or diffusion), coefficient, $D_{C_0} = 2m_1 D_C$	7.2×10^{-9} (mm^2/hr) (g/mm^3) (assuming $m_1 = 10^{-5}$ g/mm^3)
nutrient diffusion coefficient, D_n	4.6 mm^2/hr (Zhou et al. (2004))
matrix diffusion coefficient, D_m	2.5×10^{-5} mm^2/hr (Obradovic et al. (2000))
maximum stem cell proliferation rate, p_1	0.2 cell/hr or 5 cells/day (Bailón-Plaza et al. (2001))
stem cell proliferation rate, $p_{1_0} = 2m_2 p_1$	4×10^{-6} g/mm^3/hr (assuming $m_2 = 10^{-5}$ g/mm^3)
stem cell differentiation rate, p_2	3.75×10^{-3}/hr (Obradovic et al. (2000))
stem cell death rate, p_3	3.75×10^{-3}/hr (guess)
maximum chondrocyte proliferation rate, p_4	2×10^{-4}/hr (guess)
chondrocyte proliferation rate, $p_{4_0} = 2m_2 p_4$	4×10^{-9} g/mm^3/hr
chondrocyte death rate, p_5	3.75×10^{-3}/hr (guess)
matrix production rate, p_{8_0}	3.75×10^{-13}(g/mm^3)/((Nc/mm^3) hr) (Obradovic et al. (2000))
matrix degradation rate, p_{8_1}	3.75×10^{-9}/((Nc/mm^3) hr) (Obradovic et al. (2000))
nutrient uptake rate by stem cells, p_6	1.5×10^{-14}Nm/(Nc hr) (Zhou et al. (2004))
nutrient uptake rate by chondrocytes, p_7	1.5×10^{-14}Nm/(Nc hr) (Zhou et al. (2004))
maximum total cell density, C_{total,max_0}	10^6 Nc/mm^3 (assuming $10\mu m$ cell diameter)
maximum stem cell density, C_{S,max_0}	$0 - 10^6$ Nc/mm^3
maximum chondrocyte density, C_{C,max_0}	$0 - 10^6$ Nc/mm^3
maximum matrix density, m_{max}	10^{-4} g/mm^3 (Bailón-Plaza et al. (2001))
initial stem cell density, $C_S^{(0)}$	2.5×10^5 Nc/mm^3 (based on 10^6 cells in 20mm x 20mm x 10μm volume)
initial cartilage cell density, $C_C^{(0)}$	2.5×10^5 Nc/mm^3 (same as $C_S^{(0)}$)
threshold stem cell density, C_{S_0}	$C_{total,max_0}/3$ Nc/mm^3 (guess)
matrix density, m_1	10^{-5} g/mm^3 (assumed $m_{max}/10$)
matrix density, m_2	10^{-5} g/mm^3 (assumed $m_{max}/10$)
initial matrix density, m_3	10^{-8} g/mm^3 (assumed $m_{max}/10^4$)
initial nutrient concentration, N_0	$(2.85 - 9.5) \times 10^{-11}$ Nm/mm^3 (Zhou et al. (2004))
threshold nutrient concentration, n_0	2.3×10^{-11} Nm/mm^3 (Zhou et al. (2004))
critical nutrient concentration, n_1	9.5×10^{-12} Nm/mm^3 (assumed $N_0/10$)

Table 1: Estimated values of dimensional parameters. In the above, N_C represents number of cells and N_m is number of moles.

Using the above dimensionless variables, the non-dimensional equations can be written as

$$\frac{\partial \bar{C}_S}{\partial \bar{t}} = \frac{\partial}{\partial \bar{x}}\left(\bar{D}_S(\bar{m})\frac{\partial \bar{C}_S}{\partial \bar{x}}\right) + \bar{p}_1\left(\bar{m}, \frac{\bar{C}_S}{\bar{C}_{S,max}(\bar{m})}\right)\frac{\bar{n}}{\bar{n}+\bar{n}_0}\bar{C}_S H(\bar{n}-\bar{n}_1) - \bar{p}_2\bar{C}_S H\left(\bar{C}_S - \bar{C}_{S_0}\right) - \bar{p}_3\bar{C}_S H(\bar{n}_1-\bar{n}), \tag{14a}$$

$$\frac{\partial \bar{C}_c}{\partial \bar{t}} = \frac{\partial}{\partial \bar{x}}\left(\bar{D}_C(\bar{m})\frac{\partial \bar{C}_C}{\partial \bar{x}}\right) + \bar{p}_4\left(\bar{m}, \frac{\bar{C}_C}{\bar{C}_{C,max}(\bar{m})}\right)\frac{\bar{n}}{\bar{n}+\bar{n}_0}\bar{C}_C H(\bar{n}-\bar{n}_1) + \bar{p}_2\bar{C}_S H\left(\bar{C}_S - \bar{C}_{S_0}\right) - \bar{p}_5\bar{C}_C H(\bar{n}_1-\bar{n}), \tag{14b}$$

$$\frac{\partial \bar{n}}{\partial \bar{t}} = \bar{D}_n\frac{\partial^2 \bar{n}}{\partial \bar{x}^2} - \frac{\bar{n}}{\bar{n}+\bar{n}_0}\left(\bar{p}_6\bar{C}_S + \bar{p}_7\bar{C}_C\right), \tag{14c}$$

$$\frac{\partial \bar{m}}{\partial \bar{t}} = \bar{D}_m\frac{\partial^2 \bar{m}}{\partial \bar{x}^2} + \bar{p}_8(\bar{m})\frac{\bar{n}}{\bar{n}+\bar{n}_0}\bar{C}_C, \tag{14d}$$

where

$$\begin{aligned}
&\bar{p_1}\left(\bar{m}, \frac{\bar{C}_S}{\bar{C}_{S,max}(\bar{m})}\right) = A(\bar{m})\left(1 - \frac{\bar{C}_S}{\bar{C}_{S,max}(\bar{m})}\right),\ \bar{A}(\bar{m}) = \bar{p}_{1_0}\frac{\bar{m}}{\bar{m}^2+\bar{m}_2^2},\\
&\bar{p}_4\left(\bar{m}, \frac{\bar{C}_C}{\bar{C}_{C,max}(\bar{m})}\right) = \bar{B}(\bar{m})\left(1 - \frac{\bar{C}_C}{\bar{C}_{C,max}(\bar{m})}\right),\ \bar{B}(\bar{m}) = \bar{p}_{4_0}\frac{\bar{m}}{\bar{m}^2+\bar{m}_2^2},\\
&\bar{C}_{S,max}(\bar{m}) = \bar{C}_{S,max_0}(1-\bar{m}),\ \ \bar{C}_{C,max}(\bar{m}) = \bar{C}_{C,max_0}(1-\bar{m}),\ \ \bar{C}_{S,max_0} + \bar{C}_{C,max_0} = 1,\\
&\bar{p}_8(\bar{m}) = 1 - \bar{p}_{8_1}\bar{m},\ \bar{D}_S(\bar{m}) = \bar{D}_{S_0}\frac{\bar{m}}{\bar{m}^2+\bar{m}_1^2},\ \bar{D}_C(\bar{m}) = \bar{D}_{C_0}\frac{\bar{m}}{\bar{m}^2+\bar{m}_1^2}.
\end{aligned} \tag{15}$$

The non-dimensional boundary and initial conditions are

$$-\bar{D}_S(\bar{m})\frac{\partial \bar{C}_S}{\partial \bar{x}} = \bar{f}(\bar{t}),\ \ -\bar{D}_C(\bar{m})\frac{\partial \bar{C}_C}{\partial \bar{x}} = -\bar{D}_n\frac{\partial \bar{n}}{\partial \bar{x}} = -\bar{D}_m\frac{\partial \bar{m}}{\partial \bar{x}} = 0,\ \ (\text{at } \bar{x}=0), \tag{16a}$$

$$-\bar{D}_S(\bar{m})\frac{\partial \bar{C}_S}{\partial \bar{x}} = -\bar{D}_C(\bar{m})\frac{\partial \bar{C}_C}{\partial \bar{x}} = -\bar{D}_m\frac{\partial \bar{m}}{\partial \bar{x}} = 0,\ \ \bar{n}=1,\ \ (\text{at } \bar{x}=1), \tag{16b}$$

$$\bar{C}_S = \bar{C}_S^{(0)}\bar{h}(\bar{x}),\ \ \bar{C}_C = \bar{C}_C^{(0)}\bar{h}(\bar{x}),\ \ \bar{n}=1,\ \ \bar{m}=\bar{m}_3,\ \ (\text{at } \bar{t}=0), \tag{16c}$$

where $\bar{f}(\bar{t}) = f(t)/\left(p_{8_0}C_{total,max_0}^2 d/m_{max}\right)$ is a non-dimensional flux of stem cells diffusing into the defect from the underlying bone.

The dimensionless parameters and their estimated values are provided in Table 2.

3. Results

Eqs. (14-16) are solved using a second order accurate finite difference scheme to discretize the spatial derivatives, keeping the time derivative continuous. The resulting differential equations are in the form of a differential- algebraic system; to solve them we have used DASSL (Brennan et al. (1996)). The parameter values used in the simulations are: $\bar{D}_{S_0} = 10^{-2}$, $\bar{D}_{C_0} = 10^{-3}$, $\bar{D}_m = 10^{-2}$, $\bar{D}_n = 300$, $\bar{p}_{1_0} = 12$, $\bar{p}_2 = 1$, $\bar{p}_3 = 0.1$, $\bar{p}_{4_0} = 0.012$, $\bar{p}_5 = 0.1$, $\bar{p}_6 = 10^4$, $\bar{p}_7 = 10^4$, $\bar{p}_{8_1} = 1$, $n_0 = 0.24$, $n_1 = 0.1$, $m_1 = 0.1$, $m_2 = 0.1$, $m_3 = 10^{-4}$, $\bar{C}_{S_0} = 0.35$, $\bar{C}_S^{(0)} = 0.25$, $\bar{C}_C^{(0)} = 0.25$, $\bar{C}_{S,max_0} = 0.6$ and $\bar{C}_{C,max_0} = 0.4$. The initial stem cell density profile is $\bar{C}_S(x,0) = \bar{C}_S^{(0)}[1-\tanh(A(\bar{x}-\bar{x}_0))]/2$, with $A = 10^4$ and $\bar{x}_0 = 0.1$. Dimensionally, this corresponds to a stem cell density, 2.5×10^5 cells/mm^3, confined to a region of thickness 200μm near $x=0$, and zero everywhere else. In addition, stem cells migrate (or diffuse) into the defect from the subchondral bone interface ($x=0$). This flux of stem cells, $f(t)$, is assumed to exponentially decay in time. Its initial

value is taken to be between $1 - 10^2$ cells/mm^2/hr. As mentioned previously, this decrease of stem cells implies regeneration of the subchondral bone.

We first simulate the evolution of chondrocytes, matrix and nutrients in the absence of stem cells. Panel 1 in Figure 2 illustrates the protocol followed. Initially, only chondrocytes are seeded close to the subchondral bone side of the defect ($x = 0$), and the nutrient concentration is uniform. Figures 2-4 show the evolution of the chondrocyte density, C_C ($\times 10^6$ cells/mm^3), matrix density, m ($\times 10^{-4}$ g/mm^3), and nutrient concentration, n ($\times 10^{-11}$ moles/mm^3), for time ranging between 11 days to 36 months. The main features of the evolution process are as follows. At early time, chondrocytes seeded near $x = 0$ produce matrix, and consequently the matrix density there increases (panel 2 in Figure 2). The nutrient concentration at this end decreases as they are consumed by the chondrocytes. The chondrocyte proliferation rate is very low ($\bar{p}_{4_0} = 0.012$), so its subsequent evolution is primarily by diffusion. As the chondrocytes diffuse towards the end $x = d$, they produce matrix resulting in a gradual increase in matrix density throughout the defect (Figure 3). The availability of a sufficient supply of nutrients results in a rapid increase in the matrix density (Figure 4). The chondrocyte density decreases as its growth is limited by the growing matrix. The matrix and chondrocytes gradually diffuse to a steady state (panel 3 in Figure 4), with the matrix almost filling-up the entire defect.

dimensionless parameters		estimated value
stem cell migration (or diffusion) coefficient	$D_{S_0} = D_{S_0}/(p_{8_0} C_{total,max_0} d^2)$	10^{-3} - 10^{-2}
chondrocyte migration (or diffusion) coefficient	$D_{C_0} = D_{C_0}/(p_{8_0} C_{total,max_0} d^2)$	10^{-3}
nutrient diffusion coefficient	$D_n = D_n m_{max}/(p_{8_0} C_{total,max_0} d^2)$	$(1-3) \times 10^2$
matrix diffusion coefficient	$D_m = D_m/(p_{8_0} C_{total,max_0} d^2)$	10^{-3}-10^{-2}
stem cell proliferation rate	$\bar{p}_{1_0} = p_{1_0}/(p_{8_0} C_{total,max_0})$	12
stem cell differentiation rate	$\bar{p}_2 = p_2 m_{max}/(p_{8_0} C_{total,max_0})$	1
stem cell death rate	$\bar{p}_3 = p_3 m_{max}/(p_{8_0} C_{total,max_0})$	1
chondrocyte proliferation rate	$\bar{p}_{4_0} = p_{4_0}/(p_{8_0} C_{total,max_0})$	0.012
chondrocyte death rate	$\bar{p}_5 = p_5 m_{max}/(p_{8_0} C_{total,max_0})$	1
matrix degradation rate	$\bar{p}_{8_1} = p_{8_1} m_{max}/p_{8_0}$	1
nutrient uptake rate by stem cells	$\bar{p}_6 = p_6 m_{max}/(p_{8_0} N_0)$	10^4
nutrient uptake rate by chondrocytes	$\bar{p}_7 = p_7 m_{max}/(p_{8_0} N_0)$	10^4
threshold nutrient concentration	$\bar{n}_0 = n_0/N_0$	0.24-0.81
critical nutrient concentration	$\bar{n}_1 = n_1/N_0$	0.1
threshold stem cell density	$C_{S_0} = C_{S_0}/C_{total,max_0}$	0.35
initial stem cell density	$\bar{C}_S^{(0)} = C_S^{(0)}/C_{total,max_0}$	0.25
initial chondrocyte density	$\bar{C}_C^{(0)} = C_C^{(0)}/C_{total,max_0}$	0.25
maximum stem cell density	$C_{S,max_0} = C_{S,max_0}/C_{total,max_0}$	0-1
maximum chondrocyte density	$C_{C,max_0} = C_{C,max_0}/C_{total,max_0}$	0-1
matrix density	$\bar{m}_1 = m_1/m_{max}$	10^{-1}
matrix density	$\bar{m}_2 = m_2/m_{max}$	10^{-1}
initial matrix density	$\bar{m}_3 = m_3/m_{max}$	10^{-4}

Table 2: Estimated values of dimensionless parameters.

We now show the results when stem cells are present. Figures 5-7 show the evolution of the stem cell density, C_s ($\times 10^6$ cells/mm^3), chondrocyte density, C_c ($\times 10^6$ cells/mm^3), matrix density, m ($\times 10^{-4}$ g/mm^3), and nutrient concentration, n ($\times 10^{-11}$ moles/mm^3), for time ranging between 11 days to 36 months. Panel 1 in Figure 5 illustrates the protocol followed. Initially, only stem cells are seeded close to the subchondral bone side of the defect ($x = 0$), and the nutrient concentration is uniform. At early time, the stem cell density near $x = 0$ gradually increases due a combination of proliferation by uptake of nutrients and diffusion from

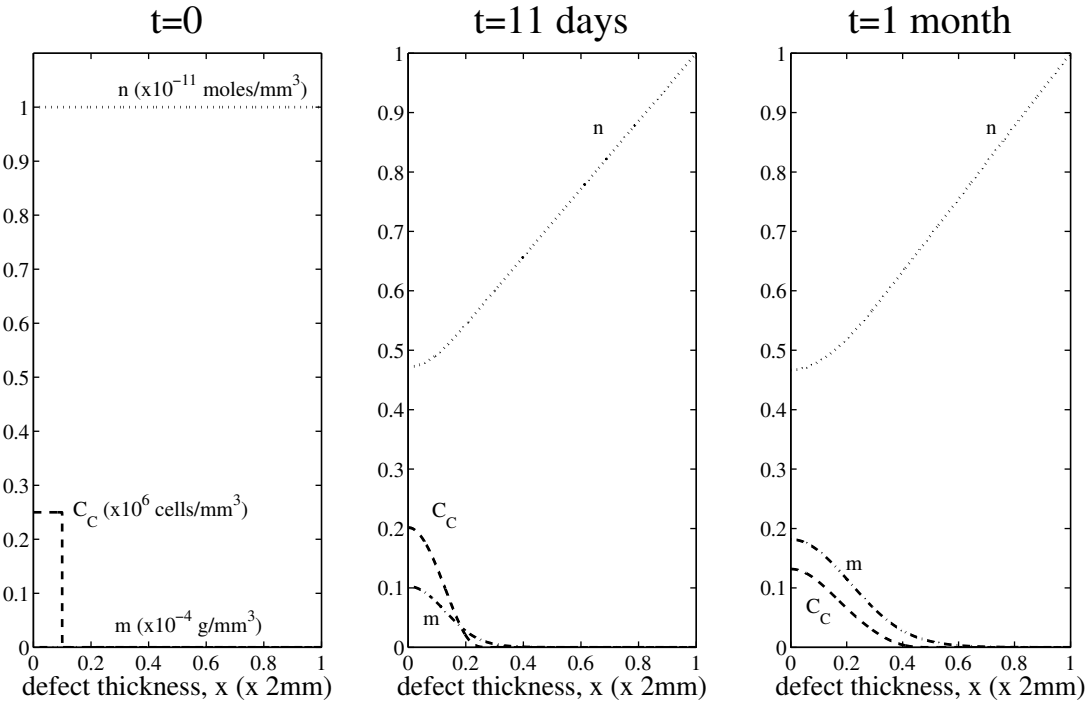

Figure 2: Evolution of chondrocyte density, C_C ($\times 10^6$ cells/mm^3), matrix density, m ($\times 10^{-4}$ g/mm^3), and nutrient concentration, n ($\times 10^{-11}$ moles/mm^3) for time, t =0, 11 days and 1 month. The initial condition at $t = 0$ corresponds to the scenario where only chondrocytes are implanted at the bottom of the defect (relevant to ACI therapy).

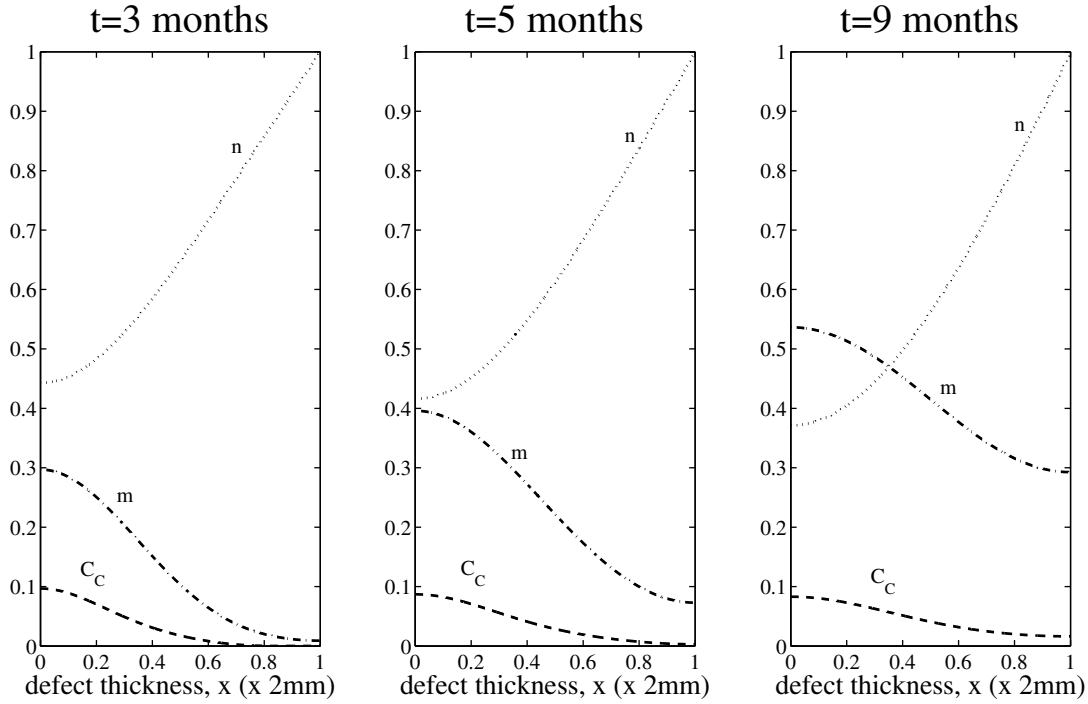

Figure 3: Evolution of cell and matrix densities, and nutrient concentration at intermediate time, t =3, 5, 9 months.

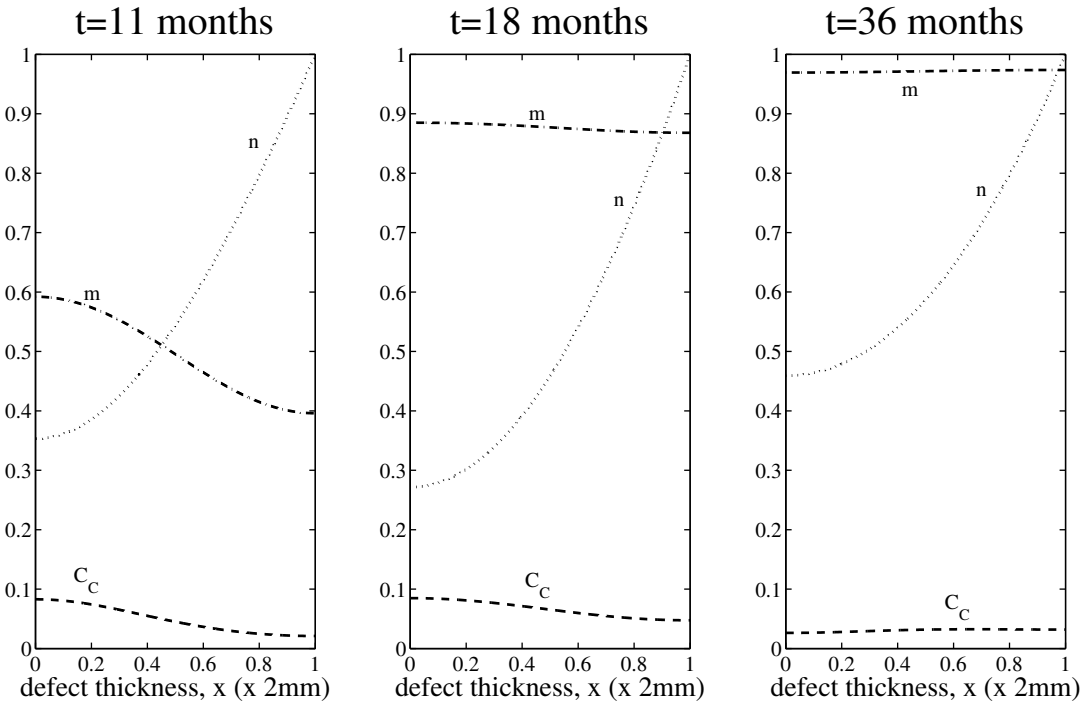

Figure 4: Evolution of cell and matrix densities, and nutrient concentration at later time, t =11, 18, 36 months.

the subchondral bone (panel 2 in Figure 5). Consequently, the chondrocyte density increases near this end mainly due to stem cell differentiation into chondrocytes, when the stem cell density exceeds the threshold value ($C_{S0} = 0.35 \times 10^6$ cells/mm^3 - panel 2 in Figure 5). The nutrient concentration near this end gradually decreases as they are consumed by the proliferating stem cells. Once the nutrient concentration falls below the critical concentration, $n_1 = 0.1 \times 10^{-11}$ moles/mm^3, the stem cell density is observed to decrease due to cell death because of low nutrient levels (panel 3 in Figure 5). A diffusion front in the stem cell density is observed to propagate to the other end, $x = d$ (panel 3 in Figure 5, panel 1 in Figure 6). A peak in stem cell density is observed precisely where the nutrient concentration exceeds its critical value (panel 3 in Figure 5, panel 1 in Figure 6). As this peak in stem cell density exceeds the threshold value for stem cell differentiation into chondrocytes, consequently a peak in the chondrocyte density is observed (panel 1 in Figure 6). The increase in chondrocyte density results in the production of matrix, hence an increase in the matrix density (panel 1 in Figure 6). As the stem cell density front reaches the defect end $x = d$, the proliferation of stem cells is enhanced due to the abundance of nutrients available (between 2 and 3 months and not shown here). The ensuing increase in stem cell density results in increase in chondrocyte density due to stem cell differentiation into chondrocytes (panels 2, 3 in Figure 6, panel 1 in Figure 7). This results in production of matrix, hence increasing the matrix density there (panels 2, 3 in Figure 6, panel 1 in Figure 7). Moreover, the abundance of nutrients available at this end also assists in the production of matrix. The stem cell and chondrocyte densities gradually decrease as their growth is limited by the growing matrix. The matrix, stem cells and chondrocytes gradually diffuse to a steady state (panels 2 and 3 in Figure 7), with the matrix almost filling-up the defect.

The growth process is also investigated for a variety of initial conditions and parameter values. Coefficients that we believe the model and application are most sensitive to are described in detail below. Sensitivity of other parameters are briefly discussed in Table 3.

Varying the initial stem cell or chondrocyte seeding density is observed to marginally enhance the produc-

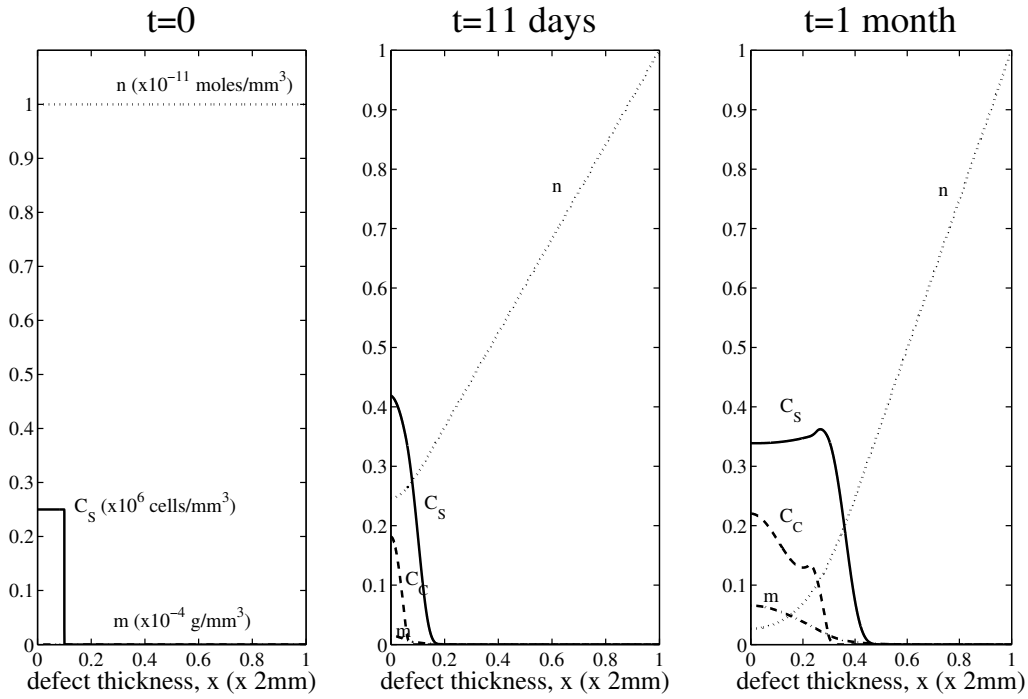

Figure 5: Evolution of stem cell density, C_s ($\times 10^6$ cells/mm^3), chondrocyte density, C_C ($\times 10^6$ cells/mm^3), matrix density, m ($\times 10^{-4}$ g/mm^3), and nutrient concentration, n ($\times 10^{-11}$ moles/mm^3) for time, t =0, 11 days and 1 month. The initial condition at $t = 0$ corresponds to the scenario where only stem cells are implanted at the bottom of the defect (relevant to ASI therapy).

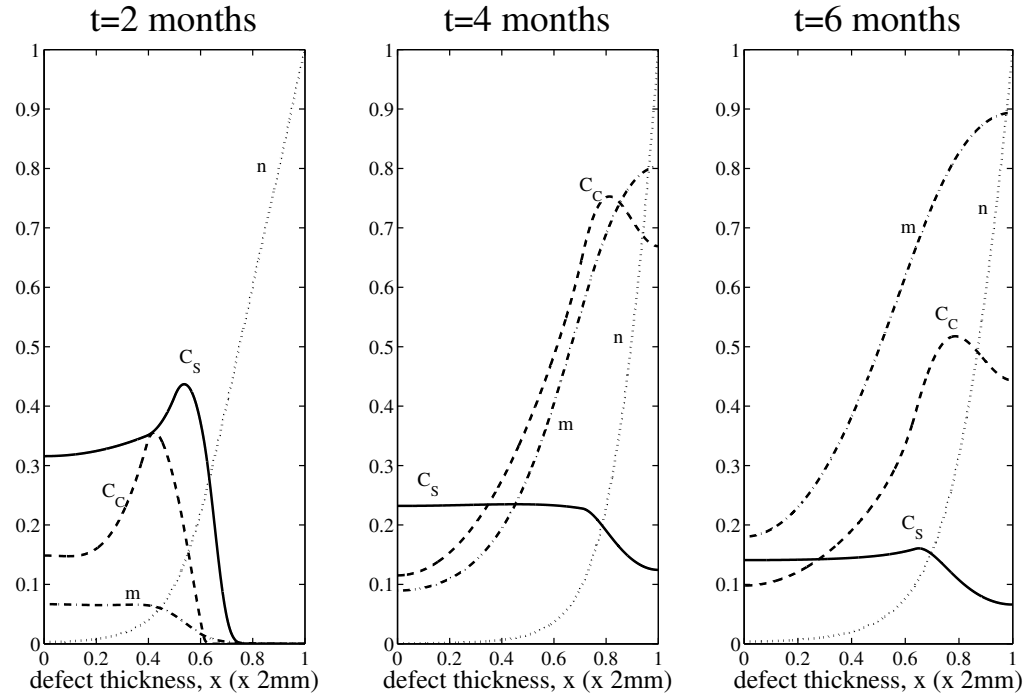

Figure 6: Evolution of cell and matrix densities, and nutrient concentration at intermediate time, t =2, 4, 6 months.

parameters	sensitivity description
initial chondrocyte seeding density	increasing this resulted in increased matrix production initially at bottom of defect; marginal enhancement in matrix production at intermediate and late times; general evolution unchanged; values used and further details in text; compare Figure 2 and Figure 8, with initial chondrocyte density doubled
initial stem cell seeding density	increasing this allowed stem cells to proliferate past threshold density for differentiation into chondrocytes sooner; slightly accelerated growth and increased density of chondrocytes and matrix; further details in text; compare Figures 5,6 and Figures 9,10, with initial stem cell density doubled
chondrocyte proliferation rate	increasing this results in a well-developed diffusive front in the chondrocyte density at intermediate time; increased proliferation of chondrocytes results in larger levels of matrix production and steady state being attained much earlier; general evolution characteristics remain unchanged; values used and further details in text; compare Figures 2-4 and Figures 11,12, with the proliferation rate increased by a factor of 100
stem cell proliferation, differentiation rate	variations only resulted in differences in magnitude of cell and matrix densities and accelerated growth; general evolution characteristics remain unchanged
cell and matrix diffusion (or migration) coefficients	influences propagation speed of diffusive front and overall time to steady state; general evolution characteristics remain unchanged
nutrient diffusion coefficient	increasing this allows nutrients to rapidly diffuse into the defect from the top, thereby reducing the nutrient concentration gradient across the defect; increase in magnitude of cell and matrix densities due to increased nutrient availability; general evolution remains unchanged
initial nutrient concentration	decreasing this resulted in proportional reduction of cell and matrix densities; evolution characteristics qualitatively similar
nutrient uptake rate	increasing this slowed down cell proliferation; longer time to steady state
matrix degradation rate	increasing/decreasing this resulted in increase/decrease in matrix production; no change in evolution characteristics
threshold stem cell density for differentiation	increasing this results in stem cells taking longer to differentiate and hence there is a delay in chondrocyte and matrix production (see Figure 13; compare with Figures 5-7 with lower threshold value); see details in text
maximum reference stem cell/chondrocyte density	increasing this allowed stem cells to proliferate to larger density; hence increased chondrocyte production after stem cell differentiation, and matrix production; values used and further details in text; compare Figures 5, 6 and Figures 14, 15; evolution at late time unchanged
stem cell flux diffusing from underlying bone	increasing/decreasing this resulted in increase/decrease in chondrocyte and matrix production; qualitative behaviour unchanged

Table 3: Sensitivity description of parameters. Those highlighted in bold are further described in the text. Their evolution characteristics are also shown in Figures 8-15.

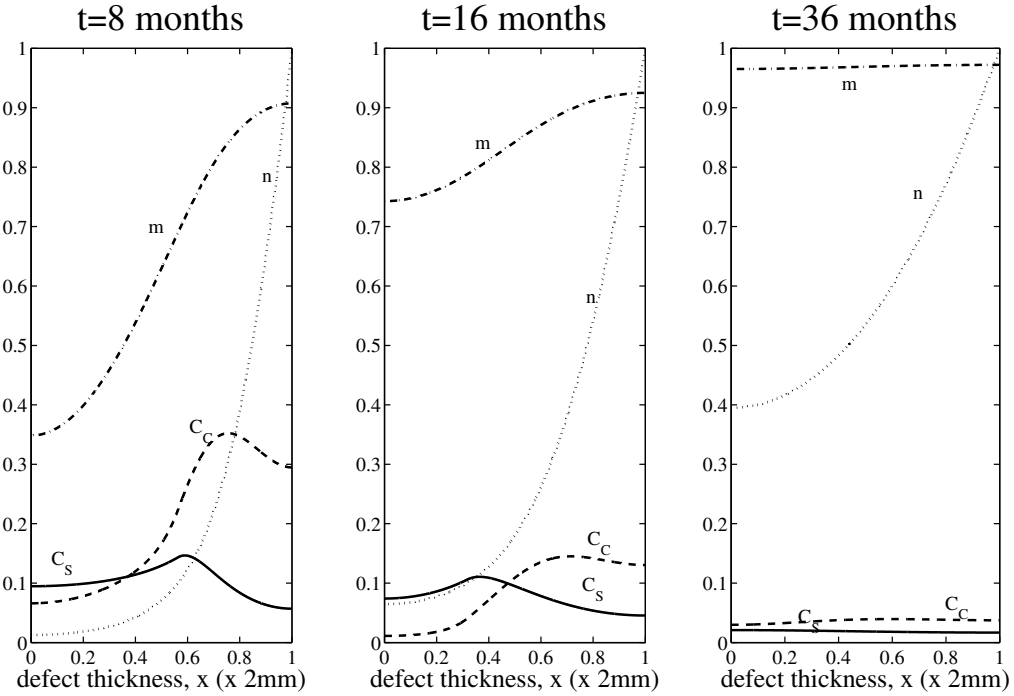

Figure 7: Evolution of cell and matrix densities, and nutrient concentration at later time, t =8, 16, 36 months.

tion of matrix, but the evolution is similar to the above cases. For example, Figure 8 shows that, in the case without stem cells, increasing the initial chondrocyte density to twice the value used in the previous simulation resulted in production of more matrix initially at the end $x = 0$ (compared to the case shown in Figure 2). However, the increase in matrix density is not substantial, its production rate being limited by the availability of nutrients, which in this case is much lower compared to the case shown in Figure 2. This is due to the increased chondrocyte density which now consumes more nutrients. The evolution beyond 1 month is similar to the previous case and is hence not shown here. In the case including stem cells, increasing the initial stem cell density to twice the value used in the previous case allowed the stem cells to proliferate past the threshold density for differentiation into chondrocytes much sooner compared to the case shown in Figure 5 (see panels 2,3 in Figure 9). Figures 9 and 10 show the resulting production of chondrocytes and matrix between 11 days to 6 months, which is slightly accelerated and has higher cell densities compared to the case shown in Figures 5-7. Hence, increasing the initial stem cell seeding density slightly accelerated the growth and increased the density of chondrocytes and matrix, however, the evolution characteristics remain unaffected.

Variations in the cell proliferation coefficients are also investigated. Only the case in the absence of stem cells is shown, the case in the presence of stem cells is similar. Figures 11,12, show the evolution for time ranging between 11 days to 3 months when the chondrocyte proliferation rate $\bar{p}_{4_0} = 1.2$ (hundred times the value used in the previous simulations). The evolution after 3 months is similar to the previous case. The evolution is almost similar to corresponding simulations in Figures 2-4 (with $\bar{p}_{4_0} = 0.012$), except a well-developed diffusive front in the chondrocyte density develops at intermediate time (Figure 12). The peak in this front is precisely where the nutrient concentration exceeds its critical value ($n_1 = 0.1 \times 10^{-11}$ moles/mm^3). The matrix density also attains a maximum there. The increased proliferation of chondrocytes results in larger levels of matrix production compared to the case shown in Figures 2-4. The subsequent evolution, after the front reaches the end $x = d$, is similar to the previous case, and eventually attains a steady state (not shown here).

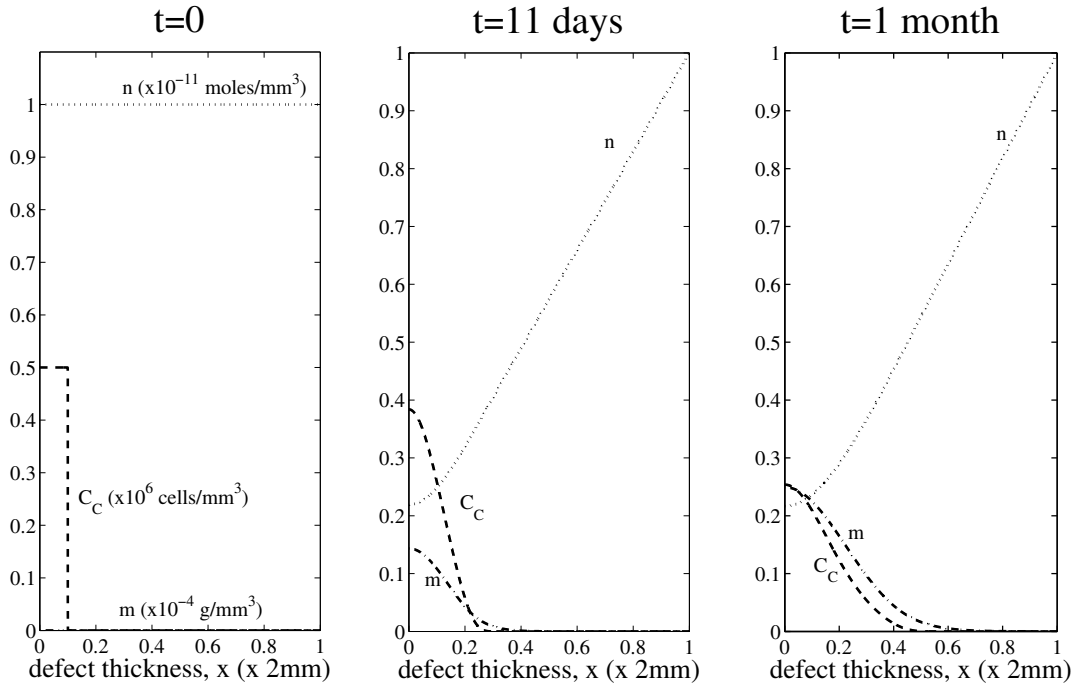

Figure 8: Evolution of chondrocyte density, C_C ($\times 10^6$ cells/mm^3), matrix density, m ($\times 10^{-4}$ g/mm^3), and nutrient concentration, n ($\times 10^{-11}$ moles/mm^3) for time, t =0, 11 days and 1 month. The initial condition at $t = 0$ corresponds to the scenario where only chondrocytes are implanted at the bottom of the defect. The initial cell density is doubled compared to the case shown in Figure 2. All other parameters are same as the case shown in Figures 2-4.

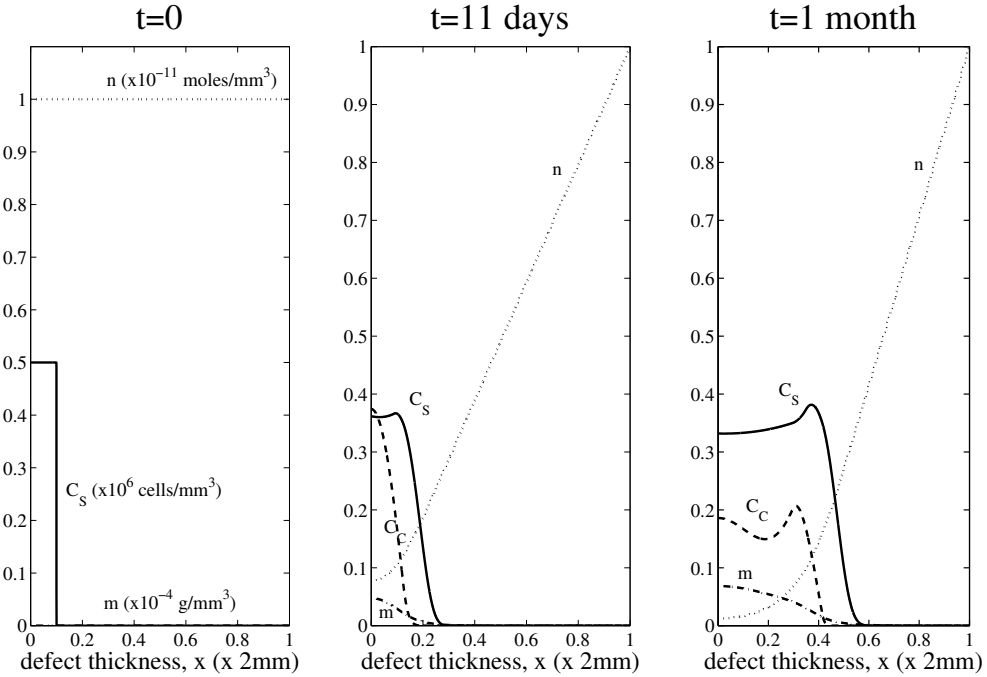

Figure 9: Evolution of stem cell density, C_s ($\times 10^6$ cells/mm^3), chondrocyte density, C_C ($\times 10^6$ cells/mm^3), matrix density, m ($\times 10^{-4}$ g/mm^3), and nutrient concentration, n ($\times 10^{-11}$ moles/mm^3) for time, t =0, 11 days and 1 month. The initial condition at $t = 0$ corresponds to the scenario where only stem cells are implanted at the bottom of the defect. The initial cell density is doubled compared to the case shown in Figure 5. All other parameters are same as the case shown in Figures 5-7.

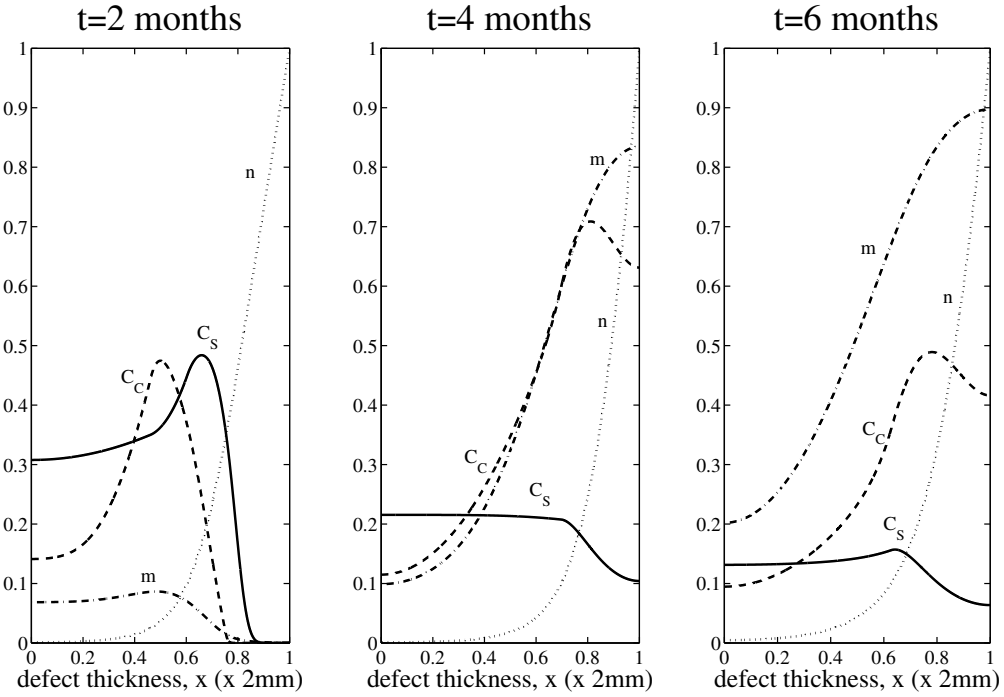

Figure 10: Evolution of cell and matrix densities, and nutrient concentration at intermediate time, t =2, 4, 6 months.

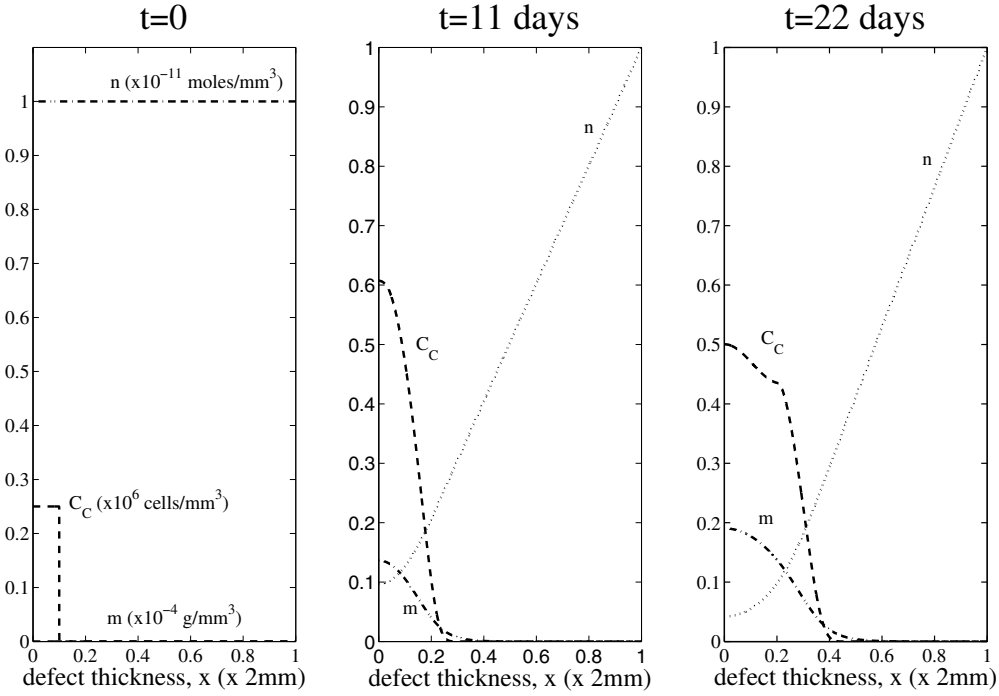

Figure 11: Evolution of chondrocyte density, C_C ($\times 10^6$ cells/mm^3), matrix density, m ($\times 10^{-4}$ g/mm^3), and nutrient concentration, n ($\times 10^{-11}$ moles/mm^3) for time, t =0, 11, 22 days. The initial condition at $t = 0$ corresponds to the scenario where only chondrocytes are implanted at the bottom of the defect. The chondrocyte proliferation rate is hundred times the value used in the case shown in Figure 2. All other parameters are same as the case shown in Figures 2-4.

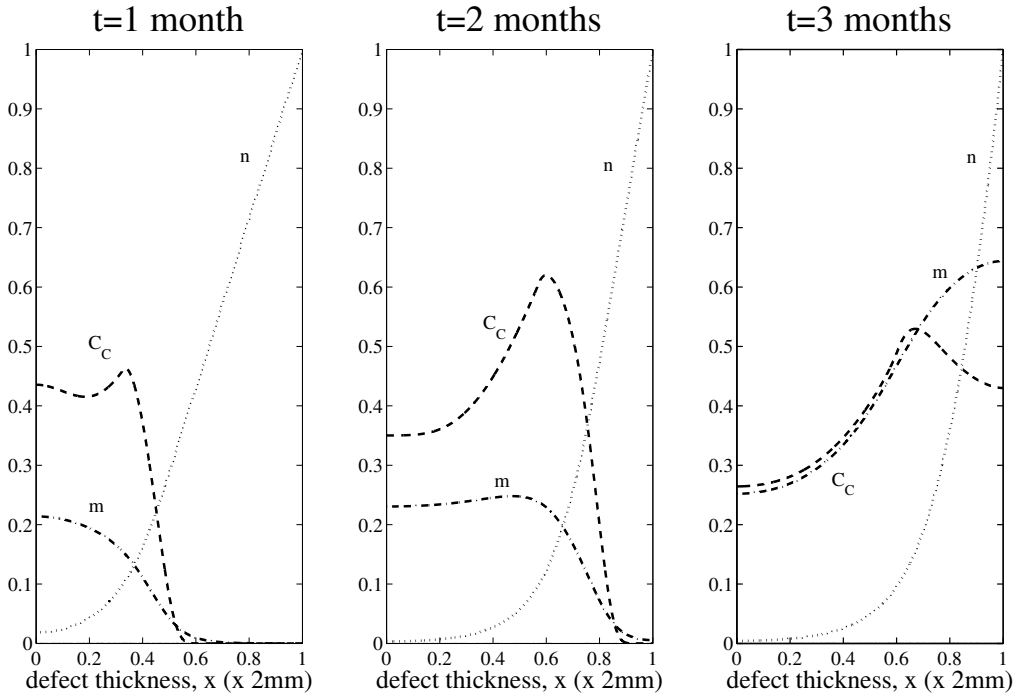

Figure 12: Evolution of cell and matrix densities, and nutrient concentration at intermediate time, t =1, 2, 3 months.

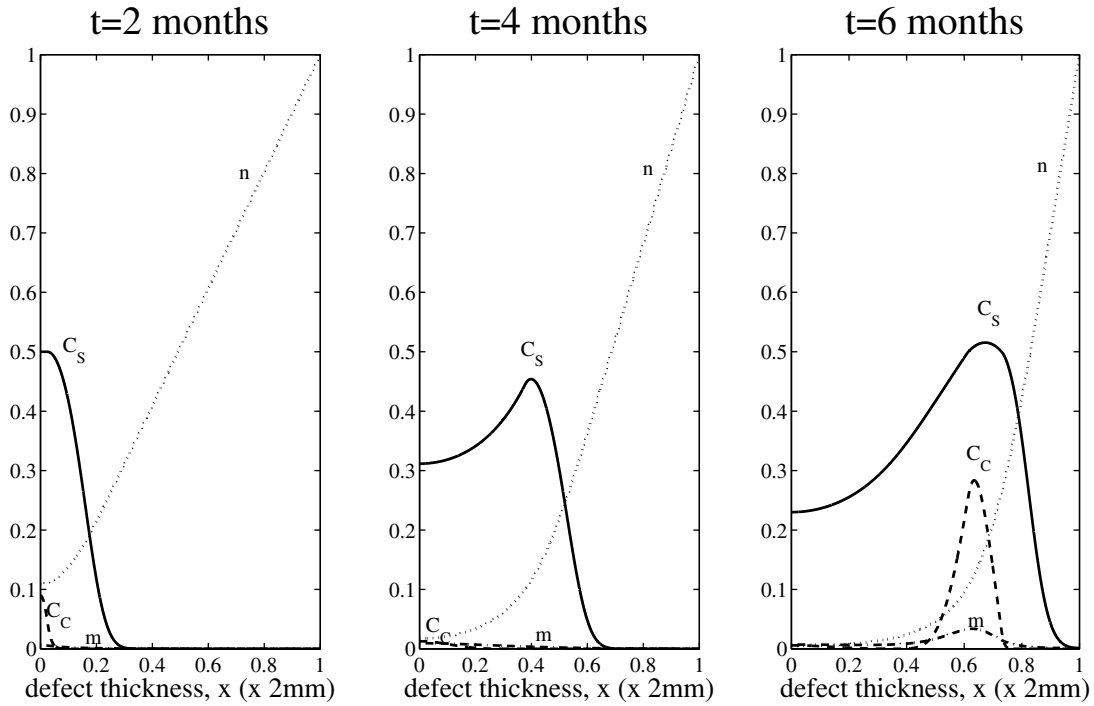

Figure 13: Evolution of cell and matrix densities, and nutrient concentration at intermediate time, t =2, 4, 6 months for the threshold stem cell density for differentiation $C_{S_0} = 0.5 \times 10^6$ cells/mm^3. All other parameters are same as the case shown in Figures 5-7.

Results varying the stem cell threshold density for differentiation, C_{S_0}, are shown in Figure 13. The value used is $C_{S_0} = 0.5 \times 10^6$ cells/mm^3 which is larger than that used to plot Figures 5-7 ($C_{S_0} = 0.35 \times 10^6$ cells/mm^3). The evolution characteristics remain generally unaffected at early and late times. However, at intermediate times (between 2-6 months), we observe a delay in the production of chondrocytes and matrix due to the diffusing stem cell density front taking longer to proliferate past the threshold value for differentiation (compare Figures 6 and 13). This delay results in the eventual filling-up of the defect with matrix taking three times longer compared to the case shown in Figures 5-7 (not shown here).

Results varying the ratio of the reference maximum stem cell and chondrocyte densities to the reference maximum total cell density, $\bar{C}_{S,max_0}$ and $\bar{C}_{C,max_0}$, respectively, are shown next. Figures 14 and 15 show the evolution between 11 days to 6 months for $\bar{C}_{S,max_0} = 0.8$ (80% of total density) and $\bar{C}_{C,max_0} = 0.2$ (20% total density). The evolution characteristics are similar to Figures 5-7, in which $\bar{C}_{S,max_0} = 0.6$ (60% of total density) and $\bar{C}_{C,max_0} = 0.4$ (40% of total density). The stem cell and chondrocyte densities are much larger, for this case, at early time (panels 2,3 in Figure 14). This is due to the stem cells being able to proliferate to a larger density and, after exceeding the threshold density for stem cell differentiation, differentiate to form chondrocytes. The larger chondrocyte density hence results in the production of more matrix (panel 3 in Figure 14 and panel 1 in Figure 15). The growing matrix limits the growth of stem cells and chondrocytes and the subsequent evolution to steady state is same as in the previous cases. Hence, increasing $\bar{C}_{S,max_0}$ well above the threshold density for stem cell differentiation results in increased chondrocyte density and hence increased matrix production. However, decreasing $\bar{C}_{S,max_0}$ below the threshold density for stem cell differentiation does not allow the stem cells to differentiate into chondrocytes, hence there are no chondrocytes or matrix produced in this case.

4. Discussion

We have formulated a simple model to explore the various processes involved in the regeneration of a cartilage defect following the implantation of chondrocytes (relevant to ACI therapy) or mesenchymal stem cells (relevant to ASI therapy). We are able to identify several growth mechanisms which allow biologically realistic growth in the stem cell, chondrocyte and matrix densities. At early time (less than 1 month), matrix production is initiated near the subchondral bone where the stem cells or chondrocytes are initially seeded. This is either due to proliferating chondrocytes producing matrix or stem cells proliferating and differentiating into chondrocytes producing matrix, both facilitated by the sufficient availability of nutrients in this region. This early-time growth mechanism is limited once the nutrient levels drop, at times, below the critical concentration for cell proliferation. At intermediate time (1-6 months), the evolution behaviour is dominated by either a chondrocyte/matrix front or a stem cell front diffusing towards the top of the defect. In the latter case, a density peak in the propagating stem cell front is observed. Once this density peak exceeds the threshold density for differentiation into chondrocytes, a local increase in chondrocyte and matrix density is observed precisely where the stem cell front peaks. The peak stem cell density front is observed where the nutrient concentration just exceeds its critical value for cell survival or where the matrix density attains a value at which the proliferation rate is maximum. Once the cell fronts reach the top of the defect, abundant availability of nutrients results in rapid cell proliferation and production of matrix. At much later time (generally between 6-18 months), the growing matrix restricts cell growth and eventually diffuses throughout the defect until it is almost completely filled.

Our model predicts that the time frame for defect repair after implantation of either chondrocyte or mesenchymal stem cells are similar. Filling-up the defect with an almost mature matrix takes approximately 16-18 months in both cases. The average matrix density levels across the defect are observed to be slightly higher in the case of stem cell implantation compared to when only chondrocytes are implanted. However, the matrix density levels are more uniform across the defect in the latter case. Moreover, the model shows large differences in chondrocyte density between both cases, with a much larger density in the stem cell implantation case. This larger density is due to the much larger proliferation rate of stem cells in comparison to

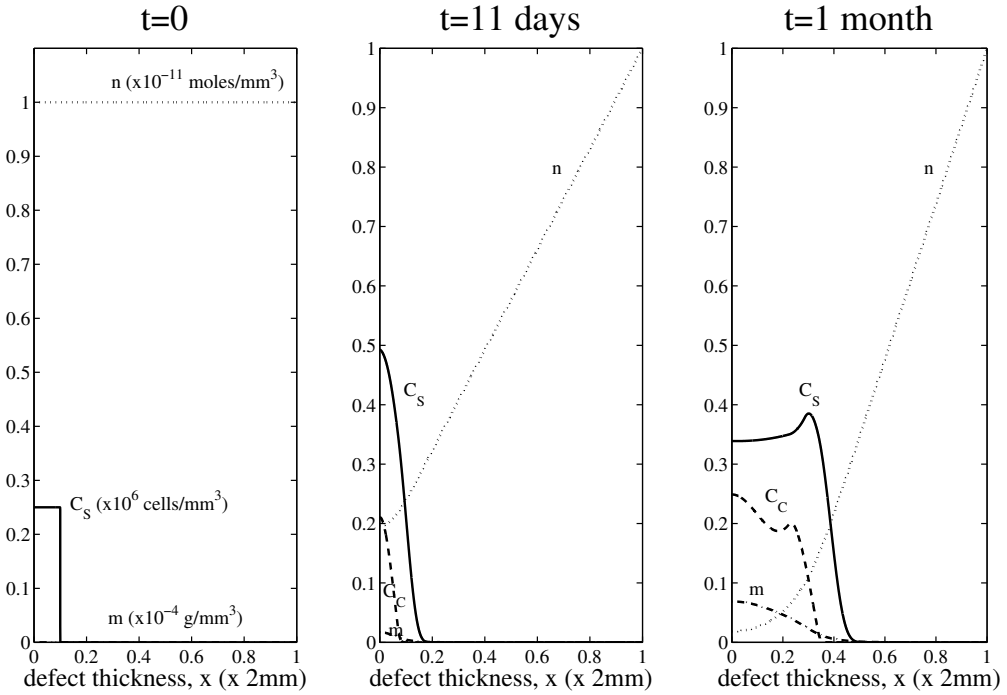

Figure 14: Evolution of stem cell density, C_s ($\times 10^6$ cells/mm^3), chondrocyte density, C_C ($\times 10^6$ cells/mm^3), matrix density, m ($\times 10^{-4}$ g/mm^3), and nutrient concentration, n ($\times 10^{-11}$ moles/mm^3) for time, t =0, 11 days and 1 month. The initial condition at $t = 0$ corresponds to the scenario where only stem cells are implanted at the bottom of the defect. In this case the reference maximum stem cell and chondrocyte densities are $\bar{C}_{S,max_0} = 0.8$ (80% of total density) and $\bar{C}_{C,max_0} = 0.2$ (20% of total density), respectively. All other parameters are the same as the case shown in Figures 5-7.

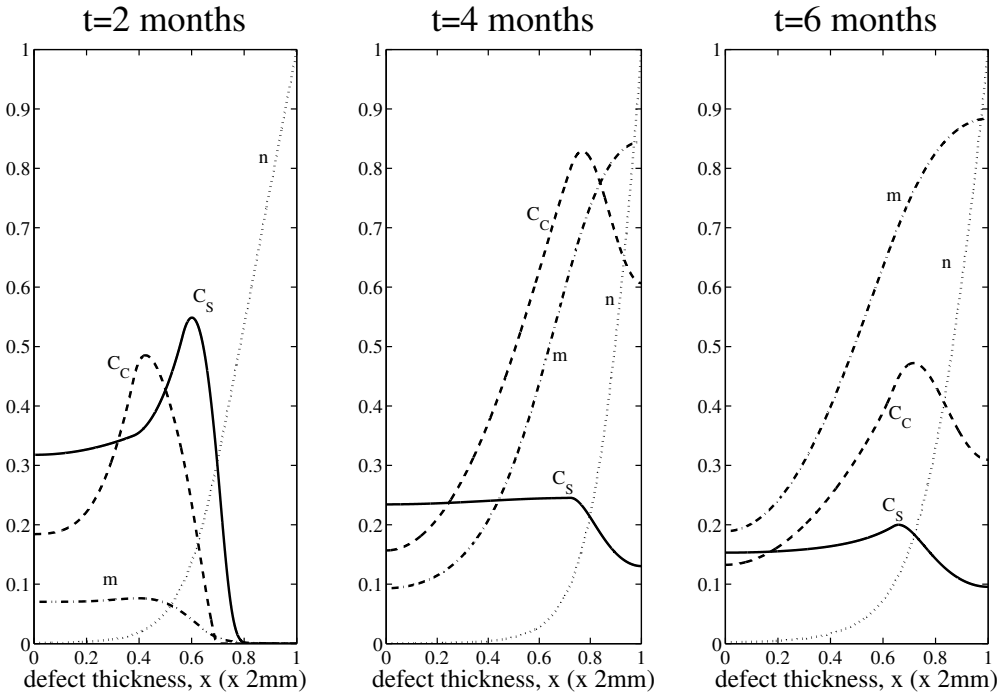

Figure 15: Evolution of cell and matrix densities, and nutrient concentration at intermediate time, t =3, 4, 6 months.

chondrocytes, which gives a high cell density before the stem cells differentiate into chondrocytes. This high chondrocyte density brings with it an excessive nutrient demand, which limits the matrix production rate. Hence, stem cell implantation might not be metabolically or nutritionally optimal compared to chondrocyte implantation. For this reason, our model suggests that stem cell implantation is no more beneficial in terms of matrix production than chondrocyte implantation. However, stem cell implantation has other benefits over chondrocyte implantation, none of them directly related to the repair, namely the avoidance of an extra surgical procedure to obtain cells, the potentially smaller donor site morbidity, and the faster proliferation rate *invitro* (Sun et al. (2010)).

Several aspects of the model predictions correspond with findings from clinical studies and animal models. The first aspect is the time frame of matrix production in our model. The time frame of 18 months for a defect to reach full maturation after chondrocyte implantation corresponds with results from a recent clinical study of patients treated with autologous chondrocytes seeded in a hyaluronan-based polymer (Brun et al. (2008)). The analysis of 70 biopsies from 63 patients in that study, taken between 5 months and 333 months after surgery, demonstrated that cartilage regeneration is a slow process taking around 18 months. Unfortunately, no further detailed data on the time course of cartilage defect healing in humans are available. However, a study on ACI using a canine model provides extensive data (Breinan et al. (1997); Breinan et al. (1998); Breinan et al. (2001)). Typically, the experiments found that the defect filled from the base (subchondral bone interface) upwards. After around 1.5-3 months, about half the thickness of the defect is filled with tissue, similar to the results of our simulation. This data suggests that the time frame of our simulation also captures the early phase of healing following ACI.

The second aspect is the difference in evolution of cell and matrix density patterns between the two cases of cell implantation considered, chondrocytes and mesenchymal stem cells. In the case of chondrocyte implantation, our model predicts a steady pattern of higher cell and matrix densities towards the bottom of the healing defect, compared to the top, while the defect gradually fills (Figures 2-4). In the case of stem cell implantation, our model predicts that after one month a moving front forms of proliferating and differentiating stem cells at the top of the defect where stem cell, chondrocyte and matrix density is largest (Figures 5-7). Such a moving front of proliferating and differentiating stem cells has also been observed in growing embryonic limb buds (Ede et al. (1975)). At intermediate time points (around nine months) average matrix density is predicted to be slightly higher after stem cell implantation than after chondrocyte implantation. Comparing these two predictions to what happens *invivo* is difficult because to our knowledge no *invivo* study has been published that directly compares cartilage repair after implanting stem cells or chondrocytes, other than two studies that used some form of scaffold, namely fibrin glue or porous polylactic acid (Hui et al. (2004); Yan et al. (2007)). A comparison across different studies is difficult due to differences in defects, species, time points and histological protocols. However, the biggest obstacle to comparing our predictions to *invivo* experiments is the use of scaffolds pre-seeded with chondrocytes or mesenchymal stem cells in the vast majority of experiments. Obviously, a proliferation/differentiation front as predicted by our model will not form in a cell-seeded scaffold. The study using fibrin glue (Hui et al. (2004)) is probably most relevant to our model, since fibrin glue has a very low density. The photomicrographs of repaired defects in that study clearly show that cell density is higher towards the top when mesenchymal stem cells had been implanted, and higher towards the bottom when chondrocytes had been implanted, in line with our predictions. Unfortunately, this study provides no quantitative information on local matrix formation. However, it does compare the indentation stiffness of the two types of repair tissues, and finds a slightly higher stiffness after stem cell implantation (Hui et al. (2004)). A study on spontaneous cartilage repair by bone marrow stromal cells of defects extending into the subchondral bone using a rabbit model provides further support to our finding of a proliferative front (Mizuta et al. (2004)). In that study, the location of proliferating mesenchymal cells in the repair tissue was assessed using an appropriate histological staining technique. These cells were mainly found at the surface of the repair tissue. On the other hand, a study of autologous chondrocyte implantation using a dog model found that "when present, chondrocytic cells were in greater numbers near the base of the lesion than in the middle or surface regions of the reparative tissue", again in accordance with the model predictions (Breinan et al. (2001)).

Finally, the finding from the current study that the initial chondrocyte density has little effect on the time course of healing or the final matrix density mirrors finding in a recent clinical study from our Institution. In that study, we found no significant effect of initial cell density on quality of repair as measured by clinical outcome (Sawkins et al. (2010)).

The model presented here also provides useful insight on the sensitivity of the growth process to the parameters involved. Varying the chondrocyte seeding density resulted in marginal changes in matrix production, in line with the clinical observations described above. Increasing the stem cell seeding density slightly accelerated the initial growth of chondrocytes and matrix, but had only little effect on the late-time evolution characteristics. Some of the other parameters proved more influential. The first of these is the chondrocyte proliferation rate. Increasing the chondrocyte proliferation rate accelerates the growth of both chondrocytes and matrix and results in steady-states being attained much earlier compared to lower proliferation rates. Similarly, increasing the stem cell proliferation and differentiation rates also accelerates the growth of chondrocytes and matrix. The model is also strongly sensitive to the threshold value of stem cell differentiation into chondrocytes. Higher values delay chondrocyte formation and matrix production and results in a longer time to steady state (almost three times longer in comparison to lower threshold values). Sensitivity to the reference maximum stem cell density is also observed to be important for the growth process. Increasing this density well above the threshold density for stem cell differentiation results in increased chondrocyte density and hence increased matrix production. However, decreasing this density below the threshold density for stem cell differentiation does not allow the stem cells to differentiate into chondrocytes, hence there are no chondrocytes or matrix produced in this case. Variations in the initial nutrient concentration only affect the magnitude of cell and matrix densities without significantly altering the timeframe to steady state. Variations in the diffusion coefficients only influence the overall time to steady state. The larger the diffusion coefficients, the faster the evolution to a steady state and vice versa.

The assumptions made in developing the current model will limit the conclusions that can be drawn from it. The two main assumptions are the dependence of stem cell differentiation into chondrocytes on cell density only, and the formation of a single type of repair tissue (cartilage). As for the first assumption, the existence of a critical cell density for stem cell differentiation to occur is well known from embryological studies of limb formation (DeLise et al. (2000)). More important for the model, the importance of a critical threshold density for differentiation to occur has also been demonstrated in transplanted human bone marrow-derived stem cells (Mankani et al. (2007)) and in spontaneous repair of small cartilage defects (Anraku et al. (2009)). Other mechanisms such as mechanical loading or growth factors (Pittenger et al. (1999)) are also important for stem cell differentiation but were neglected in the current model. Due to this limitation, the model cannot be used to address important clinical questions such as those related to patient rehabilitation or the general health state of the joint that is being treated. Secondly, only one type of repair tissue was assumed to form inside the defect, namely cartilage, characterised by a single parameter, matrix density. In reality, more types of repair tissue are found, namely fibrous tissue, hyaline cartilage and intermediate forms such as fibrocartilage (Mainil-Varlet et al. (2010)). This assumption limits the model to study the time frame of matrix formation, but not factors determining the type of tissue formed.

In conclusion, a simple model was implemented to evaluate the various processes involved in the regeneration of a cartilage defect following implantation of chondrocytes or stem cells. This model allowed us to identify typical patterns in time of cell and matrix density through the duration of the repair.

Acknowledgments

The authors acknowledge the financial support of the EPSRC research grant 3ME - Modelling Methods for Medical Engineering EP/F033125/1.

References

Ahern, B., Parvizi, J., Boston, R., Schaer, T., 2009. Preclinical animal models in single site cartilage defect testing: a systematic review. Osteoarthritis and Cartilage 17 (6), 705-713.

Anraku, Y., Mizuta, H., Sei, A., Kudo, S., Nakamura, E., Senba, K., Hiraki, Y., 2009. Analyses of early events during chondrogenic repair in rat full-thickness articular cartilage defects. Journal of Bone and Mineral Metabolism 27 (3), 272-286.

Bailón-Plaza, A., Van Der Meulen, M., 2001. A mathematical framework to study the effects of growth factor influences on fracture healing. J. Theor. Biol. 212 (2), 191-209.

Breinan, H., Minas, T., Barone, L., Tubo, R., Hsu, H.-P., Shortkroff, S., Nehrer, S., Sledge, C., Spector, M., 1998. Histological evaluation of the time course of healing of canine articular cartilage defects treated with cultured autologous chondrocytes. Tissue Engineering 4, 101-114.

Breinan, H., Minas, T., Hsu, H.-P., Nehrer, S., Shortkroff, S., Spector, M., 2001. Autologous chondrocyte implantation in a canine model: change in composition of reparative tissue with time. J. Orthopaedic Res. 19, 482-492.

Breinan, H., Minas, T., Hsu, H.-P., Nehrer, S., Sledge, C., Spector, M., 1997. Effect of cultured autologous chondrocytes on repair of chondral defects in a canine model. J. Bone and Joint Surgery 79-A, 1439-1451.

Brittberg, M. Autologous chondrocyte implantation–technique and long-term follow-up. Injury 39(1), 40-49

Brennan, K. E., Campbell, S. L., Petzold, L. E., 1996. Numerical solution of initial-value problems. SIAM, Philadelphia.

Brun, P., Dickinson, S., Zavan, B., Cortivo, R., Hollander, A., Abatangelo, G., 2008. Characteristics of repair tissue in second-look and third-look biopsies from patients treated with engineered cartilage: relationship to symptomatology and time after implantation. Arthritis Res. Ther. 10 (6), R132.

Darling, E., Athanasiou, K., 2000. Biomechanical strategies for articular cartilage regeneration. Annals of Biomedical Engineering 31 (5), 309-334.

DeLise, A., Fischer, L., Tuan, R., 2000. Cellular interactions and signaling in cartilage development. Osteoarthritis and Cartilage 8 (5), 309-334.

Ede, D., Flint, O., Teague, P., 1975. Cell proliferation in the developing wing-bud of normal and talpid3 mutant chick embryos. Journal of Embryology and Experimental Morphology 34 (3), 589.

Galban, C., Locke, B., 1997. Analysis of cell growth in a polymer scaffold using a moving boundary approach. Biotechnol. Bioeng. 56, 422-432.

Galban, C., Locke, B., 1999. Effects of spatial variation of cells and nutrient and product concentrations coupled with production inhibition on cell growth in a polymer scaffold. Biotechnol. Bioeng. 64, 633-643.

Hui, J., Chen, F., Thambyah, A., Lee, E., 2004. Treatment of chondral lesions in advanced osteochondritis dissecans: a comparative study of the efficacy of chondrocytes, mesenchymal stem cells, periosteal graft, and mosaicplasty (osteochondral autograft) in animal models. Journal of Pediatric Orthopaedics 24 (4), 427.

Jakob, M., Demarteau, O., Schafer, B., Hintermann, B., Dick, W., Heberer, M., Martin, I., 2001. Specific growth factors during the expansion and redifferentiation of adult human articular chondrocytes enhance chondrogenesis and cartilaginous tissue formation in vitro. Journal of Cellular Biochemistry 81 (2), 368-377.

Kelly, D., Prendergast, P., 2005. Mechano-regulation of stem cell differentiation and tissue regeneration in osteochondral defects. J. Biomechanics 38, 1413-1422.

Levine, H., Pamuk, S., Sleeman, B., Nilsen-Hamilton, M., 2001. Mathematical modeling of capillary formation and development in tumor angiogenesis: penetration into the stroma. Math. Biol. 63, 801-863.

Mainil-Varlet, P., Van Damme, B., Nesic, D., Knutsen, G., Kandel, R., Roberts, S., 2010. A new histology scoring system for the assessment of the quality of human cartilage repair: ICRS II. The American Journal of Sports Medicine 38 (5), 880.

Mankani, M., Kuznetsov, S., Robey, P., 2007. Formation of hematopoietic territories and bone by transplanted human bone marrow stromal cells requires a critical cell density. Experimental Hematology 35 (6), 995-1004.

Marlovits, S., Zeller, P., Singer, P., Resinger, C., Vecsei, V., 2006. Cartilage repair:generations of autologous chondrocyte transplantation. Eur. J. Radiol. 57 (1), 24-31.

McDougall, S., Anderson, A., Chaplain, M., Sherratt, J., 2002. Mathematical modeling of flow through vascular network: implications for tumor-induced angiogenesis and chemotherapy strategies. Bull. Math. Biol. 64, 673-702.

Mizuta, H., Kudo, S., Nakamura, E., Otsuka, Y., Takagi, K., Hiraki, Y., 2004. Active proliferation of mesenchymal cells prior to the chondrogenic repair response in rabbit full-thickness defects of articular cartilage. Osteoarthritis and cartilage 12 (7), 586-596.

Nejadnik, H., Hui, J., Choong, E., Tai, B., Lee, E., 2010. Autologous bone marrow-derived mesenchymal stem cells versus autologous chondrocyte implantation: an observational cohort study. Am. J. Sports Med. 38 (6), 1110-1116.

Obradovic, B., Meldon, J., Freed, L., Vunjak-Novakovic, G., 2000. Glycosaminoglycan deposition in engineered cartilage: experiments and mathematical model. AIChE J. 46 (9), 1860-1871.

Olsen, L., Sherratt, J., Maini, P., Arnold, F., 1997. A mathematical model for the capillary endothelial cell-extracellular matrix interactions in wound-healing angiogenesis. IMA J. Mathematical Medicine and Biology 14, 261-281.

Pettet, G., Byrne, H., McElwain, D., Norburry, J., 1996. A model of wound-healing angiogenesis in soft tissue. Math. Biosci. 136, 35-63.

Pittenger, M., Mackay, A., Beck, S., Jaiswal, R., Douglas, R., Mosca, J., Moorman, M., Simonetti, D., Craig, S., Marshak, D., 1999. Multilineage potential of adult human mesenchymal stem cells. Science 284 (5411), 143-158.

Roberts, S., McCall, I., Darby, A., Menage, J., Evans, H., Harrison, P., Richardson, J., 2003. Autologous chondrocyte implantation for cartilage repair: monitoring its success by magnetic resonance imaging and histology. Arthritis Res. Ther. 5 (1), R60-73.

Sawkins, M., Roberts, S., Kuiper, J.-H., Harrison, P., Robinson, E., Richardson, J., 2010. Equivalent clinical improvement after autologous chondrocyte implantation with a range of laboratory and culture parameters. Presented at the 56th Ann Meeting Orthop. Res. Soc., New Orleans, March 6-9, 2010.

Sherratt, J., Murray, J., 1990. Models of epidermal wound healing. Proc. Royal Soc. Lon. B Biol. 241, 29-36.

Sun, L. and Reagan, M.R. and Kaplan, D.L., 2010. Role of cartilage-forming cells in regenerative medicine for cartilage repair. Orthopedic Research and Reviews, 2, 85-94

Vavken, P., Samartzis, D., 2010. Effectiveness of autologous chondrocyte implantation in cartilage repair of the knee: a systematic review of controlled trials. Osteoarthritis Cartilage 18 (6), 857-863.

Yan, H., Yu, C., 2007. Repair of full-thickness cartilage defects with cells of different origin in a rabbit model. Arthroscopy: The Journal of Arthroscopic and Related Surgery 23 (2), 178-187.

Zhou, S., Cui, Z., Urban, J., 2004. Factors influencing the oxygen concentration gradient from the synovial surface of articular cartilage to the cartilage-bone interface: a modeling study. Arthritis and Rheumatism 50 (12), 3915-3924.

Zhou, S., Cui, Z., Urban, J., 2007. Nutrient gradients in engineered cartilage: metabolic kinetics measurement and mass transfer modeling. Arthritis and Rheumatism 50 (12), 3915-3924.

A Mathematical Model of Cartilage Regeneration after Cell Therapy

Michael Lutianov, Shailesh Naire, Sally Roberts, Jan-Herman Kuiper

The research highlights are as follows:

- evaluation of the processes involved in the regeneration of a cartilage defect
- identification of typical spatial and temporal patterns in time of cell and matrix density
- the model predicts a time frame of about 18 months for the defect to reach full maturation
- regeneration using stem cells alone is no better than that using chondrocytes
- with chondrocytes alone, the matrix seems to develop from the subchondral bone interface